INTRODUCTION

Heavy metals are of great concern not only among the scientific community, especially chemists, biologists and environmentalists, but also increasingly among the general population who are aware of some of the dangers associated with them. Among them, mercury is one of the most hazardous and ubiquitous pollutants released through natural events or human activities. Some microorganisms produce methyl mercury, a potent neurotoxin, from other forms of mercury that poses serious health problems by damaging central nervous and endocrine systems, leading to many cognitive and motion disorders.. The multiple pathways of spreading mercury through air, food, and water are a serious concern because it persists in the environment and subsequently bioaccumulates through the food chain. Therefore, the analysis of mercury content in water sources is a top concern of scientists.

Several methods, including atomic absorption spectroscopy, inductively coupled plasma atomic emission spectrometry, electrochemical sensing and the use of piezoelectric quartz crystals make it possible to detect low concentrations of Hg^{2+} ions. However, these methods require expensive equipment and involve time-consuming and laborious procedures that can only be carried out by trained professionals.

Alternatively, analytical techniques based on fluorescence detection are easy to perform and inexpensive and fluorescence measurements are usually very sensitive. Furthermore, the photophysical properties of a fluorophore can be easily tuned using a range of techniques such as charge-, electron-, energy-transfer, and so on. Therefore, the fluorescent sensors have been attracting the attention of many scientists.

In Vietnam, fluorescent sensors have been studied by Duong Tuan Quang since 2007. He and his co-workers reported calix[4]arene-based sensors for detection of Fe^{3+}, F^-, Cs^+ and Cu^{2+}; 1,2,3-triazoles-

based sensors for detection of Al^{3+}; and rhodamine-based sensors for detection of Hg^{2+}.

Up to now, the synthesis of fluorescent sensors is based on different fluorophores such as derivatives of rhodamine, dansyl, fluorescein, calixarene...The derivatives of rhodamine and fluorescein have been used a lot. This is because they have not only high absorption coefficient but also high fluorescence emission in the visible region and high fluorescence quantum yield. At present, there are no fluorescent sensors based on rhodamine derivatives, fluorescein that have been studied from theoretical aspect to emperically direct the design and synthesis of sensors for detection of Hg^{2+} to increase sensitivity, selectivity and to reduce the cost.

From what have been presented above, some fluorescent sensors for determination of Hg^{2+} with high sensitivity and selectivity are going to be designed and synthesized.

Therefore, we choose a research entitled "***Design and synthesis of some fluorescent sensors for determination of*** Hg^{2+}".

Chapter 1. OVERVIEW

1.1. Overview of fluorescent sensors

1.1.1. Situation of studies on fluorescent sensors

1.1.2. Operating principles of fluorescent sensors

1.1.3. Structure of fluorescent sensors

1.1.4. Principles for designing fluorescent sensors

1.2. Sources of pollution, toxicities and methods for detection of Hg(II) ion

1.3. Fluorescent sensors for detection of Hg(II) based on a spirolactam ring-opening reaction of rhodamine derivative

1.4. Fluorescent sensors for detection of Hg(II) based on a spirolactam ring-opening reaction of fluorescein derivative

1.5. Overview of application of computational chemistry in the study on fluorescent sensors

1.5.1. Application of computational chemistry in the study on structure and properties of substances

1.5.2. Application of computational chemistry in the study on reactions

Chapter 2. RESEARCH CONTENTS AND METHODS

2.1. Research objectives

- Obtaining sensors (chemosensors, chemodosimeters) for determination of Hg^{2+} based on the spirolactam ring-opening reaction of rhodamine derivative.
- Obtaining chemodosimeters for determination of Hg^{2+} based on lactam ring opening of fluorescein derivative.

2.2. Research contents

- Study on the design, synthesis, and application of rhodamine derivatives-based chemodosimeter **RT** for selective detection of Hg(II) ions.
- Study on the design, synthesis, and application of rhodamine derivatives-based chemosensor **RS** for selective detection of Hg(II) ions.
- Study on the design, synthesis, and application of fluorescein derivatives-based chemodosimeter **FS** for selective detection of Hg(II) ions.

2.3. Research methods

2.3.1. Theoretical calculation methods

- The stable geometric structures and single-point energies are determined by DFT method at B3LYP/LanL2DZ, using Gaussian 03 software.
- The corrected interaction energy parameters including enthalpy variation and Gibbs free energy variation are calculated on the basis of the difference between the total energy of products and that of the reactants.
- The excited states and the time-dependent factors are determined by TD-DFT methods at the same level of theory.
- The AIM and NBO analyses are carried out at the same level of theory (B3LYP/LanL2DZ).

2.3.2. The experimental methods

- The compounds are characterized by ^{1}H-NMR, ^{13}C-NMR, mass spectra.

- Properties, applications of the sensors are examined by fluorescence and absorption spectroscopy.

2.3.3. Other method

- Statistics

Chapter 3. RESULTS AND DISCUSSION

3.1. Design, synthesis, characteristics, and application of chemodosimeter RT for detection of Hg(II) based on a spirolactam ring-opening reaction of rhodamine derivative

3.1.1. Theoretical design, synthesis, characteristics and application of chemodosimeter RT

3.1.1.1. Survey on the calculation method

The survey on fluorescent sensors with rhodamine as a fluorophore is usually calculated with the basis function 6–311++G (d, p), this is due to the agreement between calculation results and experimental data previously reported on the structure of rhodamine – 6G according to single crystal XRD diffraction analysis. The basis function LanL2DZ is chosen for the calculations because it can reduce computation time, but still gives reliable results. Comparison of bond lengths, bond angles of **Rhd** which are calculated with two sets of function 6–311++G (d, p), LanL2DZ shows that it is possible to use the function LanL2DZ instead of 6–311++G (d, p).

3.1.1.2. Survey on the theory for design and synthesis of chemodosimeter RT

To design a suitable structure for a chemodosimeter based on ring-opening/ring-closure reaction of derivative rhodamine 6G, ethylendiamine and 4 – nitrophenyl isothiocyanate.

To predict the possibility for the synthetic reactions of **RT** to occur in terms of thermodynamics, we calculate enthalpy and Gibbs

free energy, the calculated thermodynamic parameters performed at B3LYP/LanL2DZ show $\Delta G < 0$ and $\Delta H < 0$. Therefore, in terms of thermodynamics, the synthetic reactions of chemodosimeter **RT** are likely to occur and they are exothermic.

The AIM analysis indicates that there is still a spirolactam ring in **RT**. For **RG**, the spirolactam ring is broken (C10···C22···C21···C20···N19) and there is a ring formation of 1, 3, 4 – oxadiozole (N19···C32···C33···N34···C35).

3.1.1.3. Theoretical studies of optical properties of chemodosimeter RT

a. Molecular structure of chemodosimeter RT

The optical properties of a compound depend on their molecular structures; therefore it is very necessary to study the molecular structure of chemodosimeter **RT**. The comparison of the calculation results shows that there are not significant changes in bond length, bond angle, dihedral angle of **Rhd**, **NPITC** in **RT** and those in the initial free state; the first benzene ring of xanthene contains a flexible π conjugated system; however, the π conjugated system in the second benzene ring of xanthene is not flexible.

b. UV-Vis spectral analysis of chemodosimeter RT

The UV-Vis spectra of **Rhd**, **RT** and **RG** are determined by TD-DFT method at B3LYP/LanL2DZ show that their absorption maxima appear at 473.3 , 543.6 and 476.6 nm, respectively. The electron distribution on the HOMO, LUMO of **Rhd** and **RG** is concentrated in xanthene moiety. For **RT**, the electron distribution on the HOMO is also concentrated in xanthene, but that on LUMO is mainly concentrated in **NIPTC**. These results indicate that the optical properties of **RG** should be similar to those of **Rhd**. Therefore, the expectantly designed chemodosimeter **RT** will operate on OFF-ON style.

c. Analysis of the fluorescence properties of chemodosimeter RT

Fluorescent properties of a compound depend much on π conjugation level and the energy transfer in the system.

Table 3.6. *Excitation energy, oscillation strength and MO related to the excitation of **RT** and **RG** at B3LYP / LanL2DZ*

Compound	Main orbital transition	MO	E (eV)	λ (nm)	*f*	*CIC*
RT	$S_0 \rightarrow S_1$	163→164	2,13	581,79	0,0003	0,7065
	$S_0 \rightarrow S_2$	162→164	2,28	543,63	0,0003	0,7064
	$S_0 \rightarrow S_3$	160→164	2,52	492,60	0,0002	0,6106
RG	$S_0 \rightarrow S_1$	159→160	1,79	691,58	0,0009	0,7060
	$S_0 \rightarrow S_2$	155→161	2,60	476,55	0,5727	0,12553
		159→161	2,60	476,55	0,5727	0,5797
	$S_0 \rightarrow S_3$	159→162	2,69	460,23	0,0102	0,7018

To understand the ability of a sensor to fluoresce, NBO and TD-DFT were analyzed before and after the sensor reacts with the analytes. Data in Table 3.6 and Figure 3.11 shows that the first excited state of **RT** ($S_0 \rightarrow S_1$) at 581.8 nm, corresponding to the transition MO163 → MO164 does not cause the fluorescence. This is due to the fact that MO163 belongs to the fluorophore, while MO164 belongs to the receptor; therefore the space distance between them is large, preventing the fluorescence. It is similar to the Förster Resonance Energy Transfer (FRET) - based sensors. The next excited states ($S_0 \rightarrow S_2$, $S_0 \rightarrow S_3$), corresponding to transitions MO162 → MO164 and MO160 → MO164 do not cause the fluorescence in **RT**. Here, the PET process from fluorophore to receptor occurs in **RT** because there is an MO belonging to the fluorophore with energy level between the MO of the transition. On the other hand, the transitions in **RT** ($S_0 \rightarrow S_1$, $S_0 \rightarrow S_2$, $S_0 \rightarrow S_3$) have small oscillation strength ($f < 0.01$), indicating that there is no overlap of the initial and last MOs in each transition; therefore it will not lead to the fluorescence.

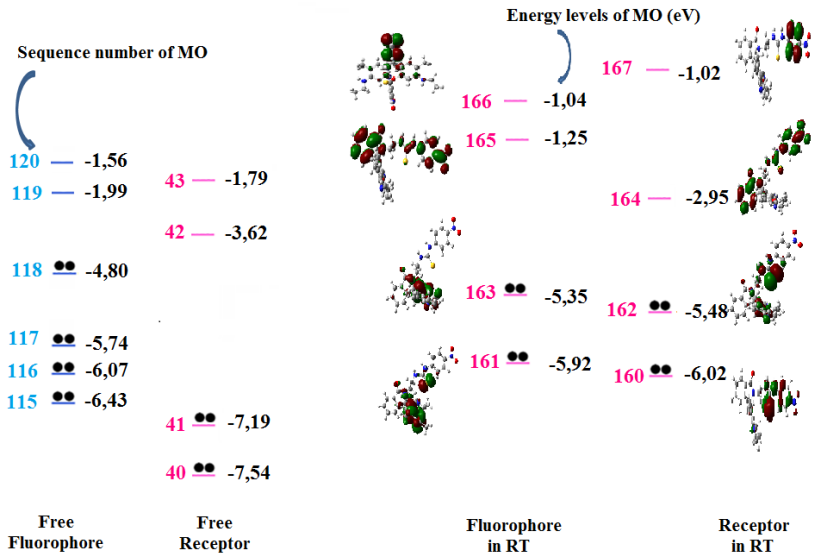

Figure 3.11. Frontier orbital energy diagram of free fluorophore, receptor and chemodosimeter **RT**

The data from Table 3.6 and Figure 3.12 shows that the first excited state of **RG** ($S_0 \rightarrow S_1$) at 691.6 nm corresponds to transition MO159 → MO160, in which MO159, MO160 belong to the fluorophore. This transition has a small oscillation strength (f = 0.0009), therefore the recovery to the ground state does not cause the fluorescence. The second excited state ($S_0 \rightarrow S_2$) corresponds to two transitions MO155 → MO161 and MO159 → MO161; for MO155 → MO161 transition, MO of the fluorophore is located between MOs of the transition, therefore PET from the fluorophore to receptor happens, and this transition will not cause the fluorescence; for MO159 → MO161 transition, because of the strong oscillation strength (f = 0.5727) and no MO of the receptor located between MOs of the transition, PET from receptor to fluorophore do not happen, and this transition causes the fluorescence in **RG**.

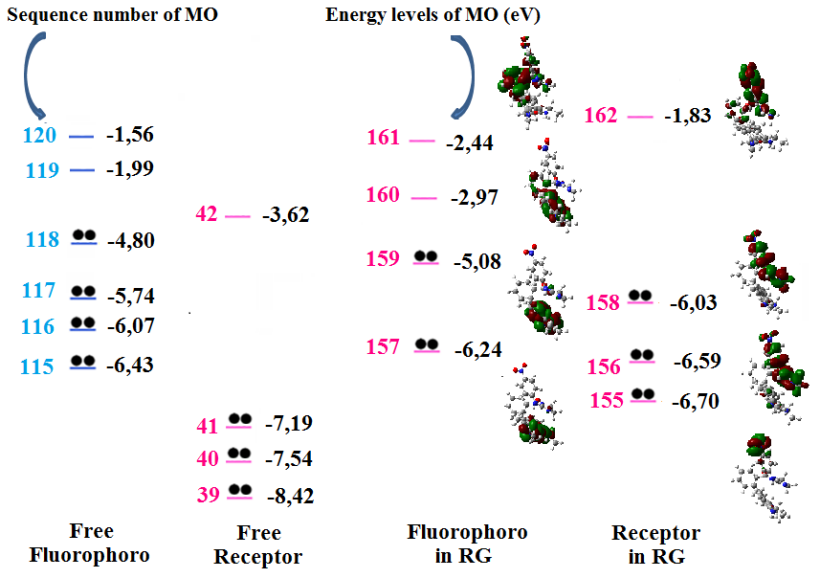

Figure 3.12. Frontier orbital energy diagram of free fluorophore, receptor and chemodosimeter **RG**

To further understand the fluorescent properties of **RT** and **RG**, NBO analysis was carried out for these compounds at the B3LYP/LanL2DZ level of theory. The results shows that **RT** has two π conjugated systems which are interrupted in the xanthene moiety of fluorophore, therefore **RT** does not cause the fluorescence. In **RG**, because the spirolactam is broken, creating a π conjugated system in fluorophore, resulting in the fluorescence in **RG**.

3.1.2. Synthesis, properties and application of chemodosimeter RT

3.1.2.1. Synthesis of the chemodosimeter RT

Synthesis of *N*-(rhodamine-6G)lactam-ethylenediamine (Rhd – E):

Rhodamine 6G (1.44 g) and ethylenediamine (2.0 mL) were mixed in 50 mL of absolute ethanol and refluxed for 4 hours till the fluorescence of the mixture solution disappeared. The reaction was cooled to room temperature and the precipitate was filtered and washed with cold ethanol for several times. The crude product was further purified by recrystallization in acetonitrile to obtain the

desired product (1.03 g, white solid) in 75.1% yield. The structure of RT is determined by ^{1}H-NMR ($CDCl_3$) and TOF – MS spectrum.

Synthesis of RT: *N*-(rhodamine-6G)lactam-ethylenediamine (456 mg) and 4-nitrophenyl isothiocyanate (270 mg) were combined in water-free acetonitrile (40 mL). The reaction solution was refluxed for 6 hours under N_2 atmosphere and stirred for another 2 hours at room temperature to give a yellow precipitate. The solid was then filtered, washed with acetonitrile for several times, dried over anhydrous $MgSO_4$ and concentrated under reduced pressure. The condensed solution was further purified by column chromatography on silica gel to give the desired product **RT** (335 mg, yield: 52.6%) as a yellow solid. The structure of **RT** is determined by ^{1}H-NMR ($CDCl_3$) and TOF – MS spectrum.

3.1.2.2. Survey on experimental applications of chemodosimeter RT

a. Absorption and fluorescence spectra of chemodosimeter RT in the presence of Hg^{2+}

The fluorescent titration spectra of solution **RT** (10μM) by Hg^{2+} shows that the fluorescence intensity of **RT** solution increases upon the addition of Hg^{2+} from 0 to 30μM. This result shows that **RT** can be used to determine Hg^{2+}.

b. Survey on reaction between chemodosimeter RT and Hg^{2+}

Job's method was used to determine the reaction stoichiometry. The result shows that **RT** reacts with Hg^{2+} in a 1: 1 ratio. Notably, addition of 2 equiv of EDTA to the solution obtained after **RT** reacts with Hg^{2+}, does not induce any further changes, indicating that the reaction is irreversible. **RT** can act as a fluorescent chemodosimeter.

c. Competitive effects of metal ions

Absorption and fluorescence spectra of RT have no distinct change upon the addition of metal ions including Zn^{2+}, Cu^{2+} , Cd^{2+}, Pb^{2+}, Ag^{+}, Fe^{2+}, Cr^{3+}, Co^{3+}, Ni^{2+}, Ca^{2+}, Mg^{2+}, K^{+} and Na^{+}. The presence of these ions does not affect the reaction between Hg^{2+} and **RT**. This experiment shows that **RT** can detect selectively Hg^{2+} in the presence of metal ions mentioned above.

d. Reaction time between Hg^{2+} and chemodosimeter RT

Reaction time between Hg^{2+} and **RT** is also surveyed. Hg^{2+} reacts almost completely with **RT**, within 5 minutes after adding Hg^{2+}, the fluorescence of **RT** solution virtually unchanged. This reaction is much faster than those of the fluorescent sensors which were previously reported.

e. Using chemodosimeter RT for quantitative detection of Hg^{2+}

The relationship between the concentration of Hg^{2+} and the fluorescence intensity of **RT** - Hg^{2+} solution was investigated. In the range of Hg^{2+} concentration from 0.1 to 25μM (respectively 20.1 ppb to 5.0 ppm), there is a good linear relationship between the variation of fluorescence intensity of **RT** and Hg^{2+} concentration, as represented by the equation: $I_{560} = (-5.80 \pm 2.86) + (1.32 \pm 0.17) \times [Hg^{2+}]$, with t_{table} (0.95; 12) = 2.17; R = 0.9982 (N = 14, P <0.0001). This shows that **RT** can be used to quantitatively detect Hg^{2+}. Limit of detection and limit of quantification for Hg^{2+} are 0.04 and 0.14 μM.

f. Influence of pH

The survey on the influence of pH shows that in the range of pH from 5 to 10, the fluorescence intensity of **RT** is minimum and virtually unchanged, while the fluorescence intensity of aqueous solution of **RT** + Hg^{2+} is maximum with no significant change. Therefore, **RT** can be used to detect Hg^{2+} in aqueous solution with fairly wide pH range from 5 to 10.

3.2. Design, synthesis, characteristics and applications of fluorescent chemosensor RS for the selective detection of Hg^{2+} based on spirolactam ring-opening of Rhodamine derivative

3.2.1. Theoretical design, synthesis, characteristics and applications of fluorescent chemosensor RS

3.2.1.1. Theoretical design and synthesis chemosensor RS

To design a chemosensor based on spirolactam ring-opening reaction, rhodamine-6G, ethylendiamine and 4-diethylaminosalicylaldehyde (**DASA**) were chosen a fluorophore,

spacer and receptor, respectively. The synthetic reactions of RS have $\Delta G < 0$, thus they are likely to occur in terms of thermodynamics.

3.1.1.2. Optical properties of chemosensor RS

a. Molecular structure of chemosensor RS

Molecular structure of chemosensor **RS** is similar to that of chemodosimeter **RT**, there is a spirolactam ring in the molecule. AIM analysis also shows that in the molecule **RS**, at the contact of **Rhd-E** and **DASA**, there is a presence of a BCP for the bond N64···C65. Besides, in the molecule RS, there is also a presence of a RCP for the bond C10···C22···C21···C20···N19. This indicates that it contains a spirolactam ring (C10···C22···C21···C20···N19) in **RS**, making the π conjugated system in fluorophore interrupted.

b. UV-Vis spectral analysis of chemosensor RS

UV-Vis spectra of **RhD** and **RS** are defined by TD-DFT method at B3LYP / LanL2DZ. The results show that the UV-Vis spectra of **RhD** and **RS** have absorption maxima at 473.3 nm and 357.9 nm, respectively; while the electrons in the HOMO, LUMO of **RhD** are mainly distributed in xanthene moiety. For **RS**, the electrons in the HOMO and LUMO are mainly distributed in the receptor. This result leads to an expectation that the optical properties of **RS** are different from those of **Rd.**

c. Fluorescence properties of chemodosimeter RS

Excitation energy and shape of Frontier MO of the receptor and **RS** are calculated by TD-DFT method at B3LYP/LanL2DZ theory, the results is summarized in the Table 3.10. It shows that with **RS**, Although the first excited state ($S_0 \rightarrow S_1$) at 426.5 nm, corresponding to two transitions MO169 → MO170, MO169 → MO171 has a large oscillation strength (f = 0,0628), it does not cause the fluorescence in **RS**, because this is an isomerization of the C = N bond. The second excited state ($S_0 \rightarrow S_2$) at 387.6 nm has a small oscillation strength (f = 0.0628), therefore this transition will not cause the fluorescence. The next excited state ($S_0 \rightarrow S_3$) at 357.9 nm, corresponding to transitions MO167 → MO170, MO167 → MO171, MO168 → MO170 and MO168 → MO171 has a large oscillation strength (f =

0,0628). In which transitions MO167 → MO170 and MO168 → MO170 do not lead to fluorescence due to FRET; MO167 → MO171, MO168 → MO171 also do not lead to fluorescence due to PET.

Table 3.2. *Excited energy, oscillation strength, and MOs related to the primary excitation of RS at B3LYP/LanL2DZ.*

Compound		MO	E (eV)	λ (nm)	F	CIC
RS	$S_0 \rightarrow S_1$	169→170	2,91	426,5	0,00628	0,64541
		169→171				-0,10360
	$S_0 \rightarrow S_2$	169→170	3,20	387,6	0,007	0,13303
		169→171				0,69201
	$S_0 \rightarrow S_3$	167→170	3,46	357,9	0,0216	0,12660
		167→171				-0,31220
		168→170				-0,46031
		168→171				-0,34850

NBO analysis shows that **RS** has two π-conjugated systems that are interrupted in the xanthene moiety of the fluorophore. This is due to the existence of a spirolactam ring in the RS that causes the C10 atom to be in the sp^3 hybridization state. It leads to the collapse of π system. As a result, there is no fluorescence in **RS**.

NBO and TD-DFT analysis shows that **RS** does not fluoresce. This is because of a presence of a spirolactam ring in **RS**, making the π conjugated system to be interrupted, and because of the isomerization of the C = N bond. Therefore, the expected chemosensor **RS** will operate in the OFF-ON mode.

3.2.2. Synthesis, characterization and application of chemosensor RS

3.2.2.1 Synthesis of chemosensor RS

456 mg of N- (rhodamine-6G) lactam-ethylenediamine and 212 mg of 4-diethylaminosalicylaldehyde were mixed in 30 mL of ethanol. The reaction solution was refluxed for 6 hours under nitrogen atmosphere and stirred for an additional 2 hours at room

temperature to obtain a precipitate. The precipitate was filtered, washed with ethanol several times and dried over $MgSO_4$, then purified by crystallization from absolute ethanol to obtain **RS** as white crystals (514 mg, yield: 81.2%). The structure of **RS** was confirmed by ^1H NMR spectrum and TOF-MS spectrum.

3.2.2.2. Application of chemosensor RS

a. UV-Vis spectra and fluorescence spectra of chemosensor RS in the presence of metal ions

The selectivity of the chemosensor RS was performed using a solution of RS (5 μM) in the presence of metal ions including Hg^{2+}, Pb^{2+}, Cd^{2+}, Cr^{3+}, Cu^{2+}, Zn^{2+}, Fe^{2+}, Co^{2+}, Ni^{2+}, Ca^{2+}, Mg^{2+}, Ag^{+}, K^{+} and Na^{+} (25 μM, respectively). From UV/Vis spectra of RS (5μM) (Fig. 3.30A), we can clearly observe a new absorption band centered at 530 nm in the presence of 5 equiv. of Hg^{2+} ions. In contrast, other metal ions do not lead to any distinct spectral changes. On the other hand, fluorescence spectra (Fig. 3.30B) also show a similar result, which is well consistent with that of UV/Vis spectra. Addition of only 5 equiv. Hg^{2+} ion results in an obviously enhanced fluorescence peaked at 556 nm (OFF–ON), while other metal ions including Pb^{2+}, Cd^{2+}, Cr^{3+}, Zn^{2+}, Cu^{2+}, Fe^{2+}, Co^{3+}, Ni^{2+}, Ca^{2+}, Mg^{2+}, K^{+} and Na^{+} ions do not give rise to any fluorescence increases. Further experiments for Hg^{2+}-selective sensing were performed using 5μM of RS in aqueous solution in the presence of multifarious ions including Pb^{2+},Cd^{2+},Cr^{3+},Zn^{2+},Cu^{2+},Fe^{2+}, Co^{3+},Ni^{2+}, Ca^{2+}, Mg^{2+}, K^{+} and Na^{+} ions (1 equiv., respectively). Upon addition of Hg^{2+} ions, the solution above still displays a distinctly enhanced fluorescence. Both UV/Vis and fluorescence results indicate that RS shows a good selectivity and sensitivity toward Hg^{2+} ions over other competitive ions.

b. Survey on the reaction between RS chemosensor RS and Hg^{2+}

The fluorescence titration spectra of **RS** (5 μM) with Hg^{2+} shows that **RS** can be used to determine Hg^{2+}. Addition of 2 equiv of EDTA to the solution obtained after Hg^{2+} reacts with RS induces a completely quenched fluorescence. This suggests that the reaction between **RS** and

Hg^{2+} is likely to be irreversible. **RS** can act as a fluorescent chemosensor. Job's method was used to determine the reaction stoichiometry. The result shows that **RS** reacts with Hg^{2+} in a 1: 1 ratio.

c. Survey on using chemosensor RS for the quantification of Hg^{2+}

The relationship between Hg^{2+} concentration and fluorescence intensity of **RS**- Hg^{2+} solution was investigated. In the range of Hg^{2+} concentration from 0.5 to 10 μM, there is a good linear relationship between the variation of fluorescence intensity of **RS** and Hg^{2+} concentration , as shown by the equation: I552 = 11.35 + 32.10 x [Hg2 +], with R = 0.9943 (N = 12, P <0.0001). This suggests that **RS** can be used to quantitatively detect Hg^{2+}. Limit of detection and limit of quantification are 0.13 and 0.45 μM, respectively.

d. Effects of pH

The effect of pH on the determination of Hg^{2+} was also investigated. The result shows that in the pH range from 6 to 10, the fluorescence intensity of **RS** reaches a minimum value and virtually unchanged; whereas, the fluorescence intensity of **RS** + Hg^{2+} solution get to a maximum value and there is also no significant change, suggesting that **RS** can be used to detect Hg^{2+} in the solution with a fairly wide pH range from 6 to 10.

3.2.3.2. Theoretical study on the application of chemosensor RS

a. Stable geometry of the complex RS-Hg^{2+}

The reaction stoichiometry between **RS** and Hg^{2+} was experimentally found to be 1:1. Theoretical calculation for optimized geometries of complexes at the theory level of B3LYP / LanL2DZ shows the stable complexes with coordination numbers 2 (R2), 3 (R3) and 4 (R4). The reactions to form R2, R3, R4 complexes have negative values of ΔG^0_{298}, ΔH^0_{298}, indicating that they both occur and are exothermic. However, ΔG^0_{298}, ΔH^0_{298} values of the reaction forming R4 are the most negative. Therefore, this is the prior reaction direction.

b. AIM Analysis

AIM analysis indicates that Hg^{2+} reacts with **RS** to form the complex having a coordination number of 4. In addition, there is no RCP of C10···C22···C21···C20···N19 bond, showing that there is not a spirolactam ring in R4.

c. Analysis of excitation energy, and MOs

Excitation energy and shape of Frontier MO of R4 are calculated by TD-DFT method at the theory level of B3LYP/LanL2DZ. The result is summarized in Table 3.2.

Table 3.14. Excitation energy, oscillation strength and MOs related to the primary excitation of R4 at B3LYP / LanL2DZ

Compound		MO	E (eV)	λ (nm)	*f*	*CIC*
R4	$S_0 \rightarrow S_1$	179→180	0,23	5318,7	0,0228	0,2390
	$S_0 \rightarrow S_2$	178→180	0,98	1332,5	0,0001	0,6905
	$S_0 \rightarrow S_3$	176→180	1,03	1199,1	0,0179	0,68585

The first excited state (S0 → S1), corresponding to the transition MO179 → MO180, in which MO179, MO180 are fluorophores, has a large oscillation strength (f = 0.0228); therefore, the recovery to the ground state causes the fluorescence. The second excited state (S0 → S2), corresponding to the transition MO178 → MO180 has a small oscillation strength (f = 0.0001), therefore it does not leads to the fluorescence. The third excited state (S0 → S3), corresponding to the transition MO177 → MO180, where MO177 belongs to the receptor and MO180 belongs to the fluorophore, does not lead to the fluorescence due to a long space distance. It is similar to the Förster Resonance Energy Transfer (FRET) - based sensors.

d. NBO Analysis

NBO analysis shows that the disruption of the spirolactam ring structure in R4 molecule changes C10 of RS from the hybridization of sp^3 to the sp^2 hybridization. Therefore, a π conjugated system is formed

throughout the fluorophore, resulting in the fluorescence in R4. On the other hand, the interaction energy E (2) from LP (2) O26 to LP (6) Hg58 and from LP (1) N64 to LP (6) Hg58 are relatively high (12.70 and 27.45 kcal mol^{-1}, respectively), suppressing the PET process from the electron pair of O26 and N64 to the xanthene moiety of fluorescein. NBO analysis shows that R4 is a fluorescent compound.

e. Fluorescent selectivity for metal ions

The fluorescent selectivity for Hg^{2+} compared to metal ions in the same groups such as Cd^{2+}, Zn^{2+} is explained by the reactivity and fluorescence of the compounds after reacting with the ions.

The reactions between **RS** and Cd^{2+} and Zn^{2+}, which form complexes with coordination number of 4 have negative values of ΔG, ΔH . Therefore, in terms of thermodynamics, they are exothermic and likely to occur.

AIM analysis indicates the complexation between RS and Cd^{2+}/Zn^{2+} with coordination of 4 through atoms O26, N34, O91, and O95, which have strong affinities to these metal ions. The dihedral angle between O95-N54 andO26-O91 bonds in both RS-Cd and RS-Zn complexes is 46.9°. This shows that O26, N54, O91 and O95 are not coplanar. In addition, the bond angles O91-Cd-O95 and O91-Zn-O95 in RS-Cd, and RS-Zn complexes are nearly 104.4°. This shows that Cd^{2+} and Zn^{2+} in both complexes are in sp^3 hybridization (tetrahedral). Meanwhile, the dihedral angle between O95-N54 and O26-O91 bonds in RS-Hg complex (R4) is 17.2°, indicating that O26, N54, O91 and O95 are nearly coplanar and Hg^{2+} in sp^2d hybridization (square planar). The fluorescence of compounds depends on the hybridization status of the central ions.

To gain insight into the fluorescence capability of complexes, TD-DFT analysis for RS-Cd and RS-Zn complexes were performed at the theory level of B3LYP / lanL2DZ. It shows that the excited states from $S_0 \rightarrow S_1$, $S_0 \rightarrow S_2$, $S_0 \rightarrow S_3$ of both RS-Cd and RS-Zn complexes have very low oscillator strengths; therefore, these transitions does not lead to the

fluorescence. This shows that Cd^{2+} and Zn^{2+} ions do not affect the detection of Hg^{2+}.

3.3. Design, synthesis, characterization and application of Fluorescein-based fluorescent chemodosimeter for Hg^{2+}.

3.3.1 Theoretical study of design, synthesis, characterization and application of fluorescent chemodosimeter FS

3.3.1.1. Survey on calculation method

The survey on fluorescent sensors with rhodamine as a fluorophore is usually calculated with the basis function 6-311+G(*d,p*). The basis function LanL2DZ is chosen for the calculations because it can reduce computation time, but still gives reliable results. Comparison of the bond length, bond angle and dihedral angles of Flu with two sets of function 6–311+G (*d, p*), LanL2DZ, shows that it is possible to use the function LanL2DZ instead of the function 6–311+G (*d, p*).

3.3.1.2. Survey on the theory for design and synthesis of chemodosimeter

To design a suitable structure for a chemodosimeter based on spirolactam ring-opening/ring-closure reaction, fluorescein, hydrazin and benzylthiocyanate were chosen as a fluorophore, spacer and receptor, respectively. To predict the possibility for the synthetic reactions of FS to occur in terms of thermodynamics, we calculate enthalpy and Gibbs free energy. The calculated thermodynamic parameters performed at B3LYP/LanL2DZ show $\Delta G < 0$ and $\Delta H < 0$. Therefore, in terms of thermodynamics, the synthetic reactions of chemodosimeter **FS** are likely to occur and they are exothermic.

The AIM analysis indicates that there is still a spirolactam ring in the FS molecule. For **FG** molecule, the spirolactam ring is broken and there is a ring formation of 1, 3, 4 – oxadiozole.

3.3.1.3. Theoretical studies of optical properties of chemodosimeter FS

The optical properties of a compound depend a lot on its molecular structure, thus it is very necessary to study the molecular structure of chemodosimeter **FS**. The comparison of calculation

results shows that there are not significant changes in bond length, bond angle, the dihedral angle of **Flu**, **BTC** in the **FS** and the initial free state remained almost unchanged. However, some geometric parameters have a relative change around C25 and N27. This could be explained by the fact that the C25 and N27 atoms of the **FS** corresponding to the sp^2 and sp^3 hybridizations; whereas, in the **BTC** they are in hybrid states of sp and sp^2 respectively. The molecular structure of **FS** shows that there are two π interruptions in the xanthene moiety of **FS**.

b. UV-Vis analysis of chemodosimeter FS

The UV-Vis spectra of **Flu**, **FS** and **FG** were determined by the TD-DFT method at B3LYP / LanL2DZ indicating that the UV-Vis spectrum of **Flu** reached a maximum at wavelength of 380.0 nm; **FS** reaches a maximum at 395.2 nm; **FG** peaks at 446.4 and 340.2 nm. These results showed that the UV-Vis spectra of **Flu** and **FS** were similar and reached the maximum at 380.0 nm and 395.2 nm respectively whilst the spectrum of **FG** is different from that of Flu, **FS** and peaks at 446.4 and 340.2 nm. This can be predicted that the **FS** has the same optical properties as **Flu** does, and it is different from **FG**.

c. Analysis of fluorescent characteristics of chemodosimeter FS

The excited energies and the shape of the fluorophore, receptor, **FG** and chemodosimeter **FS** were calculated according to the TD-DFT method at the theoretical level B3LYP / LanL2DZ. The result is summarized in Table 3.18.

Table 3.18 shows that the excited states in **FS** (S0 → S1, S0 → S2, S0 → S3), corresponding to transitions MO125 → MO126, MO124 → MO126, MO125 → MO127, have a small oscillation strength (f <0.01). As a result, it does not lead to fluorescence of **FS**. For **FG**, the first two excited states (S0 → S1, S0 → S2) correspond to transitions MO118 → MO122, MO121 → MO122 and MO121 → MO123, in which the MOs of the transition and MOs located between transitions belong to fluorophore. Therefore there is no PET

occurrence. On the other hand, these transitions have a large oscillation strength (corresponding to f = 0.1544 and 0.0136); therefore, the recovery to the ground state causes the fluorescence. The third excitation state (S0 → S3) with the corresponding transfer MO120 → MO122, although no PET occurs, this transition has a small oscillation strength (f = 0.0064). Therefore, the recovery to the ground state will not lead to fluorescence in **FG**.

Table 3.18. Excited energy, oscillation strength and MOs are related to the major excitation of Flu, BTC, FS and FG at B3LYP / LanL2DZ

Compound		MO	E (eV)	λ (nm)	*f*	*CIC*
FS	$S_0 \rightarrow S_1$	125→126	3,14	395,21	0,0088	0,7019
	$S_0 \rightarrow S_2$	24→126	3,40	364,32	0,0091	0,7024
	$S_0 \rightarrow S_3$	125→127	3,50	353,91	0,0006	0,7033
FG	$S_0 \rightarrow S_1$	118→122	2,78	446,40	0,1544	-0,1089
		121→122	2,78	446,40	0,1544	0,6948
	$S_0 \rightarrow S_2$	121→123	3,18	389,94	0,0136	0,7025
	$S_0 \rightarrow S_3$	120→122	3,36	369,14	0,0064	0,7034

The NBO analysis shows that **FS** has two π conjugated systems which are interrupted in the xanthene moiety of the fluorophore; therefore, **FS** is not fluorescent. In **FG**, due to the disruption of the spirolactam structure, the π conjugated system extends throughout the fluorophore, resulting in fluorescence in **FG**.

3.3.2. Experimental study on synthesis, characterization and application of chemodosimeter FS.

3.3.2.1. Synthesis of chemodosimeter FS

Synthesis of fluorescein hydrazide: 1.9 g (5 mmol) of fluorescein was dissolved in 100 mL of methanol and introduced to an excess amount of hydrazine hydrate (5 mL, 0.16 mol) and then refluxed for 10

hours. The resulting solution was then cooled down and evaporated in vacuo to yield a dark brown liquid. This liquid was recrystallized from an aqueous acetone-water solution (30/70, v / v) to obtain a light yellow solid (0.92 g, 47%). The product was checked for thin layer chromatography and recorded with ^{1}H-NMR ($CDCl_3$) and FAB-MS (M + H +) spectra.

The synthesis of FS: 1.73 g (5 mmol) of fluorescein was dissolved into 15 mL of DMF. 1.1 g (7.5 mmol) of benzyl thiocyanate was dissoled into 10 mL of DMF. The two solutions were mixed together, stirred for 48 hours at room temperature. The resulting solution was introduced into saturated NaCl to give an orange precipitate. The precipitate was filtered and washed with ethanol to obtain a light yellow solid. The product was then recrystallized from ethanol /water, yielding 1.56 grams of **FS** (63%). The product was checked with thin layer chromatography and recorded with ^{1}H-NMR and MS (MH^+) spectra.

3.3.2.2. Experimental investigation on the application of chemodosimeter FS

a. Fluorescence spectroscopy of chemodosimeter FS with Hg^{2+}

The solution of **FS** is colorless, not fluorescent, but when adding Hg^{2+} ions to the solution of FS in acetonitrile- H_2O (50/50, v/v) at pH ~ 7, the solution turns to light yellow and the solution of **FS** gives a rise to a strong fluorescence (at 537 nm, green) when excited at 509 nm.

b. Investigation on the reaction between chemodosimeter FS with Hg^{2+}

When adding different amounts of Hg^{2+} to the solution of **FS** at 0.1 μmol/L at pH = 7.0, the fluorescence intensity increases until the concentration of Hg^{2+} reaches 0.1 μmol/L, then the intensity is almost unchanged when Hg^{2+} is increased, indicating that Hg^{2+} reacts with **FS** in 1: 1 ratio. Notably, another experiment was also conducted by adding EDTA to the solution after the reaction between Hg^{2+} and **FS**, at a concentration twice the Hg^{2+} concentration. As a result, there is no change in fluorescence. This test shows that the response between **FS** and Hg^{2+} is irreversible. **FS** can act as a fluorescent chemodosimeter.

c. Investigation on the effect of competitive metal ions

Fluorescence change of **FS** solution upon the addition of different metal ions, including Ag^+, Pb^{2+}, Cd^{2+}, Cr^{3+}, Zn^{2+}, Fe^{2+}, Co^{3+}, Ni^{2+}, Ca^{2+}, Mg^{2+}, K^+, Na^+ and Hg^{2+} was carried out. It can be seen that there is a negligible increase in fluorescence intensity when Ag^+ was introduced, while the other metal ions almost do not affect the fluorescence of the FS. The high selection of **FS** for Hg^{2+} ions can be explained by the fact that the formation of HgS with very low solubility makes the **FS** open its ring more effectively. This experiment showed that **FS** could selectively detect Hg^{2+} in the presence of these above metal ions.

d. Survey on the reaction time between Hg^{2+} and chemodosimeter FS

The dependence of fluorescence intensity on the reaction time between Hg^{2+} and chemodosimeter **FS** was also investigated. Its result shows that the fluorescence signal of **FS** increased in the first 15 minutes and then the fluorescence intensity was almost unchanged.

e. Investigation on the use of chemodosimeter FS to determine Hg^{2+}

The correlation between Hg^{2+} concentration and fluorescence intensity of **FS**- Hg^{2+} was investigated. The result shows that in the Hg^{2+} concentration range from 0.2 to 3 μM, the fluorescence intensity is linearly correlated with Hg^{2+} concentration. This is expressed by the equation: $I_{537} = -4.98 + 249.61 \times [Hg^{2+}]$, with R = 0.999 (N = 12, P <0.0001). This indicates that **FS** can be used for the quantitative determination of Hg^{2+}. The limit of detection and the limit of quantification are 0.05 and 0.15 μM respectively.

f. Investigation on the effects of pH

In order to use the chemodosimeter **FS** in practical application, the effect of pH on the Hg^{2+} determination was also investigated. The result shows that the fluorescence intensity increases as the pH of the solution increases and remains nearly unchanged in the range from 6.5 and 8.5. Meanwhile, the solution containing only **FS** does not fluoresce in the surveyed pH range.

CONCLUSIONS

1. The flexible combination between quantum chemical calculations and experimental studies have been successfully applied in research and development of chemodosimeter **RT**, chemodosimeter **FS** and chemosensor **RS**. For chemodosimeter **RT**, **FS**, calculations predict and orientate all processes; then experimental research will verify and confirm the calculated results. For chemosensor **RS**, calculations are used to predict and orientate stages of experimental design, synthesis and characterization; besides, calculations are used to explain the experimental results related to the detection of Hg^{2+}. This flexible combination significantly reduces the volume of theoretical calculations and experiments, increasing the likelihood of success, saving time and cost of chemicals used.

2. Chemodosimeter **RT**, chemodosimeter **RT** and chemosensor **RS** have been successfully synthesized from rhodamin and fluorescein derivatives. These chemodosimeters and chemosensor are characterized by ^{1}H-NMR, ^{13}C-NMR and mass spectra. Chemodosimeter **RT** shows a fluorescent emission maximum at 560 nm when excited at 530 nm wavelength. Chemodosimeter **FS** shows a fluorescent emission maximum at 537 nm when excited at 509 nm wavelength. Chemosensor **RS** shows a fluorescent emission maximum at 552 nm when excited at 500 nm wavelength.

3. Chemodosimeter **RT** can selectively detect Hg(II) with detection limit of 8.04 ppb and quantification limit of 28.14 ppb. Chemodosimeter **FS** can selectively detect Hg(II) with detection limit of 8 ppb and quantification limit of 30 ppb; the reactions occur almost instantaneously; pH ranges are wide, from 5 to 10 for **RT** and from 6.5 to 8.5 for **FS**; only a small amount of organic solvent is needed and the analysis proccess is not affected by other metal ions including Zn(II), Cu(II), Cd(II), Pb(II), Ag(I), Fe(II), Cr(III), Co(III), Ni(II), Ca(II), Mg(II), K(I) and Na(I). The selectivity of

chemodosimeter **RT** and chemodosimeter **FS** for Hg(II) is explained by characteristic reaction of **RT**, **FS** caused by Hg(II) - a reaction between thiourea derivative with amine leading to a guanidine cyclization in the presence of Hg(II).

4. Chemosensor **RS** can selectively detect Hg(II) ions in aqueous solution. Chemosensor **RS** has some advantages such as low detection limit and low quantitation limit, 26.13 ppb and 90.45 ppb, respectively; pH range is wide, from 5 to 10; only a small amount of organic solvent is needed; the analysis proccess is not affected by competing metal ions including Na(I), K(I), Pb(II), Cd(II), Co(II), Ca(II), Ba(II), Mg(II), Zn(II), Fe(II), Ni(II), Al(III) and Cr(III).

5. The fluorescent properties as well as the fluorescent signal changes before and after the sensors interact with analytes are studied through the analysis of excited states by TD-DFT method and the investigation on the nature of bonds from NBO analysis. Accordingly, the chemodosimeter **RT**, **FS** interacts with Hg^{2+} to cause the desulfurization and the guanidine cyclization, resulting in the lactam ring-opening, and therefore leading to the fluorescence of **RT**, **FS**. Meanwhile, chemosensor **RS** coordinates with Hg^{2+} also opens the spirolactam ring, leading to the fluorescence of **RS**.